

# Subdiffraction incoherent optical imaging via spatial-mode demultiplexing

Mankei Tsang<sup>1,2,\*</sup>

<sup>1</sup>*Department of Electrical and Computer Engineering,*

*National University of Singapore, 4 Engineering Drive 3, Singapore 117583*

<sup>2</sup>*Department of Physics, National University of Singapore, 2 Science Drive 3, Singapore 117551*

(Dated: June 15, 2019)

I propose a spatial-mode demultiplexing (SPADE) scheme for the far-field imaging of arbitrary incoherent optical sources. For an object too small to be resolved by direct imaging under the diffraction limit, I show that SPADE can estimate the moments of the source distribution much more precisely than direct imaging can fundamentally do under the effect of photon shot noise.

Recent research, initiated by our group [1–6], has shown that far-field linear optical methods can significantly improve the localization of two equal-strength incoherent optical point sources when Rayleigh’s criterion is violated [7–12], overcoming previously established limits [13–15]. An open problem, of fundamental interest in optics and monumental importance to astronomy and fluorescence microscopy, is whether these results can be generalized for arbitrary incoherent sources. Here I take the first step towards solving the problem by proposing a generalized spatial-mode demultiplexing (SPADE) scheme for the imaging of incoherent source distributions. The use of coherent optical processing to improve the lateral resolution of incoherent imaging has thus far received little attention, as conventional wisdom suggests that any improvement should be modest [16]. Using quantum optics and parameter estimation theory, here I show that, for an object too small to be resolved by diffraction-limited direct imaging, SPADE can estimate the moments of the source distribution much more precisely than direct imaging can fundamentally do in the presence of photon shot noise. Given the importance of moments to imaging in identifying the size and shape of an object [17], the proposed scheme should provide a boost to incoherent imaging applications that are limited by diffraction and shot noise [18–23].

To ensure rigor, I start with the quantum formalism established in Ref. [1]. The quantum state of incoherent light in  $M$  temporal modes can be written as  $\rho^{\otimes M}$ , where  $\rho$  can be expressed as

$$\rho = (1 - \epsilon)\rho_0 + \epsilon\rho_1 + O(\epsilon^2), \quad (1)$$

$\epsilon$  is the average photon number per mode assumed to be  $\ll 1$  [24],  $\rho_0 = |\text{vac}\rangle\langle\text{vac}|$  is the vacuum state,  $\rho_1$  is the one-photon state with its density matrix determined by the mutual coherence function, and  $O(\epsilon^2)$  denotes second-order terms, which are neglected hereafter. It is standard to assume that the fields from incoherent objects, such as stellar or fluorescent emitters, are spatially uncorrelated at the source [24]. In a diffraction-limited imaging system, the fields then propagate as waves; the Van Cittert-Zernike theorem is the most venerable consequence [24]. At the image plane of a conventional two-dimensional imaging system in the paraxial regime, this

implies

$$\rho_1 = \int d^2\mathbf{R}\Lambda(\mathbf{R})|\psi_{\mathbf{R}}\rangle\langle\psi_{\mathbf{R}}|, \quad (2)$$

$$|\psi_{\mathbf{R}}\rangle = \int d^2\mathbf{r}\psi(\mathbf{r} - \mathbf{R})|\mathbf{r}\rangle, \quad (3)$$

where  $\mathbf{R} = (X, Y)$  is the object-plane position vector,  $\Lambda(\mathbf{R})$  is the source intensity distribution with normalization  $\int d^2\mathbf{R}\Lambda(\mathbf{R}) = 1$ , and  $|\mathbf{r}\rangle = a^\dagger(\mathbf{r})|\text{vac}\rangle$  is a one-photon position eigenket on the image plane at position  $\mathbf{r} = (x, y)$  with  $[a(\mathbf{r}), a^\dagger(\mathbf{r}')] = \delta^2(\mathbf{r} - \mathbf{r}')$  [25], and  $\psi(\mathbf{r})$  is the field point-spread function (PSF) of the imaging system. Without loss of generality, the image-plane position vector  $\mathbf{r}$  has been scaled with respect to the magnification to follow the same scale as  $\mathbf{R}$  [26]. For convenience, I also normalize the position vectors with respect to the width of the PSF to make them dimensionless.

Consider the processing and measurement of the image-plane field by linear optics and photon counting. The counting distribution for each  $\rho$  can be expressed as  $\langle n_0, n_1, \dots | \rho | n_0, n_1, \dots \rangle$ , where  $|n_0, n_1, \dots\rangle = (\prod_{j=0}^{\infty} b_j^{\dagger n_j} / \sqrt{n_j!}) |\text{vac}\rangle$ ,  $b_j \equiv \int d^2\mathbf{r}\varphi_j^*(\mathbf{r})a(\mathbf{r})$ ,  $\varphi_j(\mathbf{r})$  is the optical mode function that is projected to the  $j$ th output, and  $[b_j, b_k^\dagger] = \int d^2\mathbf{r}\varphi_j^*(\mathbf{r})\varphi_k(\mathbf{r}) = \delta_{jk}$ . With the negligence of multiphoton coincidences, the relevant projections are  $\{|\text{vac}\rangle, |\varphi_j\rangle\}$ , with  $|\varphi_j\rangle \equiv |0, \dots, n_j = 1, \dots, 0\rangle = b_j^\dagger |\text{vac}\rangle = \int d^2\mathbf{r}\varphi_j(\mathbf{r})|\mathbf{r}\rangle$ . The zero-photon probability becomes  $1 - \epsilon$  and the probability of one photon being detected in the  $j$ th mode becomes  $\epsilon p(j)$ , where

$$p(j) \equiv \langle \varphi_j | \rho_1 | \varphi_j \rangle = \int d^2\mathbf{R}\Lambda(\mathbf{R}) |\langle \varphi_j | \psi_{\mathbf{R}} \rangle|^2 \quad (4)$$

is the one-photon distribution. For example, direct imaging can be idealized as a measurement of the position of each photon, leading to an image given by

$$\lambda(\mathbf{r}) \equiv \langle \mathbf{r} | \rho_1 | \mathbf{r} \rangle = \int d^2\mathbf{R}\Lambda(\mathbf{R}) |\psi(\mathbf{r} - \mathbf{R})|^2, \quad (5)$$

which is a basic result in statistical optics [24]. Over  $M$  temporal modes, the probability distribution of photon numbers  $m = (m_0, m_1, \dots)$  detected in the respective optical modes

becomes

$$P(m) = \sum_L \mathcal{M}(m|L)\mathcal{B}(L), \quad (6)$$

where  $\mathcal{B}(L)$  is the binomial distribution for detecting  $L$  photons over  $M$  trials with single-trial success probability  $\epsilon$  and  $\mathcal{M}(m|L) = \delta_{L, \sum_j m_j} L! \prod_j [p(j)]^{m_j} / m_j!$  is the multinomial distribution of  $m$  given  $L$  total photons [27]. Taking the limit of  $\epsilon \rightarrow 0$  while holding  $N = M\epsilon$  constant,  $\mathcal{B}(L)$  becomes Poisson with mean  $N$ , and  $P(m) \rightarrow \exp(-N) \prod_j [Np(j)]^{m_j} / m_j!$ , which is the standard Poisson model of photon counting for incoherent sources at optical frequencies [15, 18–24].

The central goal of imaging is to infer unknown properties of the source distribution  $\Lambda(\mathbf{R})$  from the measurement outcome  $m$ . Here I frame it as a parameter estimation problem, defining  $\theta = (\theta_1, \theta_2, \dots)$  as a vector of unknown parameters and assuming the source distribution  $\Lambda(\mathbf{R}|\theta)$  to be a function of  $\theta$ . Denote an estimator as  $\hat{\theta}(m)$  and its error covariance matrix as  $\Sigma_{\mu\nu}(\theta) = \sum_m P(m|\theta) [\hat{\theta}_\mu(m) - \theta_\mu][\hat{\theta}_\nu(m) - \theta_\nu]$ . For any unbiased estimator ( $\sum_m \hat{\theta}(m)P(m|\theta) = \theta$ ), the Cramér-Rao bound is given by [27]

$$\Sigma_{\mu\mu}(\theta) \geq [J^{-1}(\theta)]_{\mu\mu}, \quad (7)$$

where  $J(\theta)$  is the Fisher information matrix given by

$$J_{\mu\nu}(\theta) \equiv \sum_m \frac{1}{P(m|\theta)} \frac{\partial P(m|\theta)}{\partial \theta_\mu} \frac{\partial P(m|\theta)}{\partial \theta_\nu}. \quad (8)$$

The bound is asymptotically attainable using the maximum-likelihood estimator for large  $N$  [27]. The Fisher information is nowadays regarded as the standard precision measure in incoherent imaging [22, 28, 29], especially in fluorescence microscopy [15, 19–21].

To compute the information for Eq. (6), note that, for a given outcome  $m$ ,  $P(m) = \mathcal{M}(m|\sum_j m_j)\mathcal{B}(\sum_j m_j)$ , and if  $\epsilon$  is given so that  $\mathcal{B}$  does not depend on  $\theta$ , the score functions [27] with respect to  $P$  and  $\mathcal{M}$  are identical ( $\partial \ln P(m|\theta) / \partial \theta_\mu = \partial \ln \mathcal{M}(m|\sum_j m_j, \theta) / \partial \theta_\mu$ ). This means that the Fisher information, which is also given by the covariance of the score function, can be obtained by computing the information for  $\mathcal{M}(m|L, \theta)$  and then averaging it over  $\mathcal{B}(L)$ . This leads to

$$J_{\mu\nu}(\theta) = N \sum_j \frac{1}{p(j|\theta)} \frac{\partial p(j|\theta)}{\partial \theta_\mu} \frac{\partial p(j|\theta)}{\partial \theta_\nu}. \quad (9)$$

The Poisson model, being a limit of Eq. (6), naturally has the same expression for its information [13–15, 19, 21, 22]. For example, the direct-imaging information, given Eq. (5), is

$$J_{\mu\nu}^{(\text{direct})}(\theta) = N \int d^2\mathbf{r} \frac{1}{\lambda(\mathbf{r}|\theta)} \frac{\partial \lambda(\mathbf{r}|\theta)}{\partial \theta_\mu} \frac{\partial \lambda(\mathbf{r}|\theta)}{\partial \theta_\nu}. \quad (10)$$

The effect of finite-size pixels can be similarly studied by assuming  $p(j|\theta) = \int_{\mathcal{A}_j} d^2\mathbf{r} \lambda(\mathbf{r}|\theta)$ , where  $\mathcal{A}_j$  is the domain of

each pixel, although the resulting information must be lower than Eq. (10) owing to the data-processing inequality [30].

SPADE is a technique previously proposed for the purpose of estimating the separation between two incoherent point sources [1, 2, 8, 10–12]. I now ask how SPADE can be generalized for the imaging of an arbitrary source distribution. Consider the transverse-electromagnetic (TEM) basis  $\{|\mathbf{q}\rangle; \mathbf{q} = (q_x, q_y) \in \mathbb{N}^2\}$  [31], where

$$|\mathbf{q}\rangle = \int d^2\mathbf{r} \phi_{\mathbf{q}}(\mathbf{r}) |\mathbf{r}\rangle, \quad (11)$$

$$\phi_{\mathbf{q}}(\mathbf{r}) \equiv \frac{\text{He}_{q_x}(x) \text{He}_{q_y}(y)}{\sqrt{2\pi q_x! q_y!}} \exp\left(-\frac{x^2 + y^2}{4}\right), \quad (12)$$

and  $\text{He}_q$  is the Hermite polynomial [32, 33]. Assuming a Gaussian PSF given by  $\psi(\mathbf{r}) = \phi_{(0,0)}(\mathbf{r})$ , which is a common assumption in fluorescence microscopy [19, 21],  $|\psi_{\mathbf{R}}\rangle$  is a coherent state [34], and the one-photon density matrix in the TEM basis becomes

$$g(\mathbf{q}, \mathbf{q}'|\theta) \equiv \langle \mathbf{q} | \rho_1(\theta) | \mathbf{q}' \rangle \quad (13)$$

$$= C(\mathbf{q}, \mathbf{q}') \int d^2\mathbf{R} \Lambda(\mathbf{R}|\theta) e^{-(X^2 + Y^2)/4} \times X^{q_x + q'_x} Y^{q_y + q'_y}. \quad (14)$$

$$C(\mathbf{q}, \mathbf{q}') \equiv \frac{1}{2^{|\mathbf{q} + \mathbf{q}'|} \sqrt{\mathbf{q}! \mathbf{q}'!}}, \quad (15)$$

where I have introduced the shorthands

$$|\mathbf{q}| \equiv q_x + q_y, \quad \mathbf{q}! \equiv q_x! q_y!. \quad (16)$$

To investigate the precision arising from SPADE measurements, define the parameters of interest as

$$\theta_\mu = \int d^2\mathbf{R} \Lambda(\mathbf{R}|\theta) e^{-(X^2 + Y^2)/4} X^{\mu_X} Y^{\mu_Y}, \quad (17)$$

with  $\mu = (\mu_X, \mu_Y)$ , leading to a linear parameterization of  $g$  given by

$$g(\mathbf{q}, \mathbf{q}'|\theta) = C(\mathbf{q}, \mathbf{q}') \theta_{\mathbf{q} + \mathbf{q}'}. \quad (18)$$

Notice that each  $\theta_\mu$  is a moment of the source distribution filtered by a Gaussian. In particular, if the object is much smaller than the PSF width, the Gaussian can be neglected, and  $\theta_\mu$  becomes a moment of the source distribution itself. This subdiffraction regime is of central interest to superresolution imaging and, as shown later, also a regime in which direct imaging performs poorly. Since a distribution is uniquely determined by its moments [17],  $\Lambda(\mathbf{R}|\theta) \exp[-(X^2 + Y^2)/4]$  and therefore  $\Lambda(\mathbf{R}|\theta)$  can in principle be reconstructed given the moments. Note also that the moment order  $\mu$  is nontrivially related to the order of the matrix element via  $\mu = \mathbf{q} + \mathbf{q}'$ , and one should be careful not to confuse the theory here with the coherent imaging theory [16, 26, 35–37].

A measurement in the TEM basis yields

$$p^{(\text{TEM})}(\mathbf{q}|\theta) = C(\mathbf{q}, \mathbf{q}) \theta_{2\mathbf{q}}, \quad (19)$$

which leads to a diagonal information matrix, with

$$J_{\mu\mu}^{(\text{TEM})}(\theta) = \begin{cases} NC(\boldsymbol{\mu}/2, \boldsymbol{\mu}/2)/\theta_{\mu}, & \mu_X \text{ and } \mu_Y \text{ are even,} \\ 0, & \text{otherwise,} \end{cases} \quad (20)$$

meaning that the TEM measurements are sensitive only to moments with even  $\mu_X$  and  $\mu_Y$ . To access the other moments, consider interferometry between two TEM modes that implements the following projections:

$$|+\rangle \equiv \frac{1}{\sqrt{2}}(|\mathbf{q}\rangle + |\mathbf{q}'\rangle), \quad |-\rangle \equiv \frac{1}{\sqrt{2}}(|\mathbf{q}\rangle - |\mathbf{q}'\rangle). \quad (21)$$

This two-channel interferometric TEM (iTEM) measurement leads to

$$\begin{aligned} p^{(\text{iTEM})}(|+\rangle|\theta) &= \frac{C(\mathbf{q}, \mathbf{q})\theta_{2\mathbf{q}} + C(\mathbf{q}', \mathbf{q}')\theta_{2\mathbf{q}'}}{2} \\ &\quad + C(\mathbf{q}, \mathbf{q}')\theta_{\mathbf{q}+\mathbf{q}'}, \\ p^{(\text{iTEM})}(|-\rangle|\theta) &= \frac{C(\mathbf{q}, \mathbf{q})\theta_{2\mathbf{q}} + C(\mathbf{q}', \mathbf{q}')\theta_{2\mathbf{q}'}}{2} \\ &\quad - C(\mathbf{q}, \mathbf{q}')\theta_{\mathbf{q}+\mathbf{q}'}. \end{aligned} \quad (22)$$

The dependence on  $\theta_{\mathbf{q}+\mathbf{q}'}$  is the main interest here, as it allows one to access any moment parameter, but the probabilities also depend on a background parameter, defined as

$$\beta(\mathbf{q}, \mathbf{q}') \equiv \frac{C(\mathbf{q}, \mathbf{q})\theta_{2\mathbf{q}} + C(\mathbf{q}', \mathbf{q}')\theta_{2\mathbf{q}'}}{2}. \quad (23)$$

If  $\beta$  is known, via a prior TEM measurement for example, the single-parameter information

$$J_{\mu\mu}^{(\text{iTEM})}(\theta) = \frac{2NC^2(\mathbf{q}, \boldsymbol{\mu} - \mathbf{q})\beta(\mathbf{q}, \boldsymbol{\mu} - \mathbf{q})}{\beta^2(\mathbf{q}, \boldsymbol{\mu} - \mathbf{q}) - C^2(\mathbf{q}, \boldsymbol{\mu} - \mathbf{q})\theta_{\boldsymbol{\mu}}^2} \quad (24)$$

for  $\boldsymbol{\mu} = \mathbf{q} + \mathbf{q}'$  is a satisfactory precision measure. If  $\beta$  is unknown, however, it is necessary to consider two-parameter estimation, calculate the two-by-two information matrix, and take the inverse to obtain the Cramér-Rao bound in the presence of the nuisance parameter  $\beta$  [38]. The information with respect to  $\theta_{\mathbf{q}+\mathbf{q}'}$  in this scenario can be defined as

$$j_{\mu\mu}^{(\text{iTEM})} \equiv \frac{1}{[J^{(\text{iTEM})}]_{\mu\mu}^{-1}} = \frac{2NC^2(\mathbf{q}, \boldsymbol{\mu} - \mathbf{q})}{\beta(\mathbf{q}, \boldsymbol{\mu} - \mathbf{q})}, \quad (25)$$

which is necessarily lower than Eq. (24).

For multiparameter estimation and general imaging, multiple TEM and iTEM measurements are needed. To be specific, Table I lists a set of schemes that together can be used to estimate all the moment parameters, while Fig. 1 shows a graphical representation of the schemes in the  $(q_x, q_y)$  space. The use of neighboring modes in the proposed iTEM schemes is motivated by the fact that the  $C(\mathbf{q}, \boldsymbol{\mu} - \mathbf{q})$  factor in Eq. (25) is maximized if  $\mathbf{q}$  is as close to  $\boldsymbol{\mu} - \mathbf{q}$  as possible. The bases in different schemes are incompatible with one another, so the photons have to be rationed among the schemes, by applying

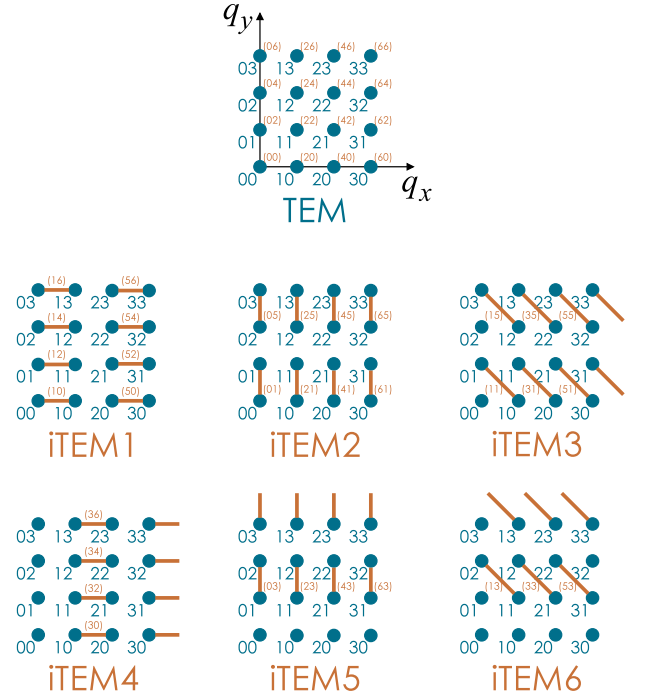


FIG. 1. Each dot corresponds to a TEM mode in the  $(q_x, q_y)$  space, and each line connecting two dots denotes an interferometer between two modes in an iTEM scheme. The bracketed numbers are the orders  $(\mu_X, \mu_Y)$  of the moment parameters to which the projections are sensitive. The unconnected dots in some of the iTEM schemes denote the rest of the modes in a complete basis, which can be measured simultaneously to provide extra information.

them sequentially through reprogrammable interferometers or spatial-light modulators [12, 37, 39, 40] for example.

Although the proposed SPADE measurements can in principle perform general imaging, their complexity would not be justifiable if they did not offer any significant advantage over direct imaging. To analyze the performance of direct imaging with a Gaussian PSF, expand  $|\psi(\mathbf{r} - \mathbf{R})|^2$  in a Taylor series to obtain

$$\lambda(\mathbf{r}|\theta) = |\phi_{(0,0)}(\mathbf{r})|^2 \left[ 1 + \sum_{\boldsymbol{\mu}} D_{\boldsymbol{\mu}}(\mathbf{r})\theta'_{\boldsymbol{\mu}} \right], \quad (26)$$

$$D_{\boldsymbol{\mu}}(\mathbf{r}) \equiv \frac{\text{He}_{\mu_X}(x) \text{He}_{\mu_Y}(y)}{\boldsymbol{\mu}!}, \quad (27)$$

$$\theta'_{\boldsymbol{\mu}} \equiv \int d^2\mathbf{R} \Lambda(\mathbf{R}|\theta) X^{\mu_X} Y^{\mu_Y}. \quad (28)$$

In terms of this parameterization, the information becomes

$$J_{\mu\nu}^{(\text{direct})}(\theta') = N \int d^2\mathbf{r} |\phi_{(0,0)}(\mathbf{r})|^2 \frac{D_{\boldsymbol{\mu}}(\mathbf{r})D_{\boldsymbol{\nu}}(\mathbf{r})}{1 + \sum_{\boldsymbol{\eta}} D_{\boldsymbol{\eta}}(\mathbf{r})\theta'_{\boldsymbol{\eta}}}. \quad (29)$$

Assume now that the support of the source distribution is centered at the origin and has a maximum width  $\Delta$  much smaller

Scheme	Projections	Mode index $q_x$	Mode index $q_y$	Moment order $\mu_X$	Moment order $\mu_Y$
TEM	$ \mathbf{q}\rangle$	$\mathbb{N}$	$\mathbb{N}$	even	even
iTEM1	$[ \mathbf{q}\rangle \pm  \mathbf{q} + (1, 0)\rangle]/\sqrt{2}$	even	$\mathbb{N}$	1, 5, 9, ...	even
iTEM2	$[ \mathbf{q}\rangle \pm  \mathbf{q} + (0, 1)\rangle]/\sqrt{2}$	$\mathbb{N}$	even	even	1, 5, 9, ...
iTEM3	$[ \mathbf{q} + (1, 0)\rangle \pm  \mathbf{q} + (0, 1)\rangle]/\sqrt{2}$	$\mathbb{N}$	even	odd	1, 5, 9, ...
iTEM4	$[ \mathbf{q}\rangle \pm  \mathbf{q} + (1, 0)\rangle]/\sqrt{2}$	odd	$\mathbb{N}$	3, 7, 11, ...	even
iTEM5	$[ \mathbf{q}\rangle \pm  \mathbf{q} + (0, 1)\rangle]/\sqrt{2}$	$\mathbb{N}$	odd	even	3, 7, 11, ...
iTEM6	$[ \mathbf{q} + (1, 0)\rangle \pm  \mathbf{q} + (0, 1)\rangle]/\sqrt{2}$	$\mathbb{N}$	odd	odd	3, 7, 11, ...

TABLE I. A list of measurement schemes, their projections, and the moment parameters to which they are sensitive.

than the PSF width, viz.,

$$\Delta \ll 1, \quad (30)$$

which defines the subdiffraction regime. The parameters are then bounded by

$$|\theta'_\mu| \leq \Delta^{|\mu|}, \quad (31)$$

and the image is so blurred that it resembles the TEM<sub>00</sub> mode rather than the object, viz.,

$$\lambda(\mathbf{r}|\theta) = |\phi_{(0,0)}(\mathbf{r})|^2 [1 + O(\Delta)]. \quad (32)$$

Equation (29) becomes

$$J_{\mu\nu}^{(\text{direct})}(\theta') = \frac{N\delta_{\mu\nu}}{\mu!} [1 + O(\Delta)]. \quad (33)$$

The small-object assumption also means that the Gaussian in Eq. (17) can be neglected, and the  $\theta_\mu$  parameters defined there becomes  $\theta'_\mu + O(\Delta^{|\mu|+2})$ . Equation (33) can then be compared with the SPADE information given by Eqs. (20) and (25). For the TEM measurement, an information enhancement factor can be defined as

$$\frac{J_{\mu\mu}^{(\text{TEM})}}{J_{\mu\mu}^{(\text{direct})}} \approx \frac{N^{(\text{TEM})}}{N^{(\text{direct})}} \frac{\mu!}{2^{|\mu|} (\mu/2)! \theta_\mu}. \quad (34)$$

Apart from a factor  $N^{(\text{TEM})}/N^{(\text{direct})}$  determined by the different photon numbers detectable in each method, the important point is that the factor scales inversely with  $\theta_\mu \leq \Delta^{|\mu|}$ , so the enhancement is enormous in the subdiffraction regime. The prefactor also increases with increasing  $\mu$ .

The information from an iTEM measurement must be at least the value given by Eq. (25), so an enhancement factor can be expressed as

$$\frac{j_{\mu\mu}^{(\text{iTEM})}}{J_{\mu\mu}^{(\text{direct})}} \approx \frac{N^{(\text{iTEM})}}{N^{(\text{direct})}} \binom{\mu}{\mathbf{q}} \frac{1}{2^{2|\mu|-1} \beta(\mathbf{q}, \mu - \mathbf{q})}, \quad (35)$$

$$\binom{\mu}{\mathbf{q}} \equiv \frac{\mu!}{\mathbf{q}!(\mu - \mathbf{q})!}. \quad (36)$$

With  $\beta(\mathbf{q}, \mu - \mathbf{q}) = O(\Delta^{\min[2|\mathbf{q}|, 2(\mu - \mathbf{q})]})$ , both  $1/\beta$  and the coefficient defined by Eq. (36) can be maximized by choosing

$\mathbf{q}$  to be as close to  $\mu/2$  as possible. This justifies the pairing of neighboring modes in the iTEM schemes listed in Table I and Fig. 1. With  $\beta = O(\Delta^{|\mu|-1})$  for odd  $|\mu|$  (using iTEM1, iTEM2, iTEM4, or iTEM5) and  $\beta = O(\Delta^{|\mu|})$  for even  $|\mu|$  (using iTEM3 or iTEM6), the enhancements can again be substantial, except for the first moments  $\theta_{(1,0)}$  and  $\theta_{(0,1)}$ , which determine the object centroid and can be well estimated by direct imaging.

These results can be compared with Refs. [1, 2] for the special case of two equal-strength point sources. If the origin of the image plane is aligned with their centroid and their separation along the  $X$  direction is  $d$ ,  $\theta_{(2,0)} \approx \theta'_{(2,0)} = d^2/4$ , and a coordinate transformation yields  $\mathcal{J}^{(\text{direct})}(d) \approx Nd^2/8$  and  $\mathcal{J}^{(\text{TEM})}(d) \approx N/4$  with respect to  $d$ , in accordance with the results in Refs. [1, 2] to the leading order of  $d$ . The experiments reported in Refs. [10–12] serve as demonstrations of the proposed scheme in this special case.

Intuitively, the enhancements can be understood by inspecting the form of the Fisher information given by Eq. (9). Consider the single-parameter information for a given  $\theta_\mu$ . The linear parameterization used here means that the mean intensity of each output,  $\propto p(j|\theta)$ , consists of a signal component  $\propto \theta_\mu$  and a  $\theta_\mu$ -independent background. To maximize the information, the background should be minimized to reduce the denominator in Eq. (9). In other words, with shot noise, it is desirable to have dark ports, as is well known in optical interferometry. In the subdiffraction regime, the background for direct imaging indicated by Eq. (26) is dominated by the TEM<sub>00</sub> mode. SPADE, on the other hand, is able to lower the background for each output by filtering out irrelevant low-order TEM modes. To wit, Eq. (19) for TEM measurements has zero background, while Eqs. (22) for iTEM also have low backgrounds in the subdiffraction regime. The surprise here is that such coherent optical processing in the far field can substantially improve incoherent imaging, without the need to manipulate the sources like prior superresolution microscopic methods [36, 41–43]. In this respect, the proposed scheme seems to work in a similar way to nulling interferometry for exoplanet detection [44, 45]. The nulling was used for the special purpose of blocking the emission of a star, however, and there had not been any prior study of nulling in the subdiffraction regime to my knowledge.

To be sure, the seemingly infinite enhancement offered by



SPADE does not imply unlimited resolution for finite photon numbers. The higher moments are still more difficult to estimate, as the fractional error  $\sim 1/(\theta_\mu^2 J_{\mu\mu})$  is  $1/O(N\Delta^{|\mu|})$  for even  $|\mu|$  and  $1/O(N\Delta^{|\mu|+1})$  for odd  $|\mu|$ , meaning that more photons are needed to achieve a satisfactory fractional error for higher  $|\mu|$ . Provided that enough photons can be collected, however, the giant improvements over direct imaging ( $1/(\theta_\mu^2 J_{\mu\mu}^{\text{direct}}) = 1/O(N\Delta^{2|\mu|})$ ) should still be useful, especially when moment parameters are of primary interest [17]. For example, by aligning a SPADE device with the centroid of a star, a planetary system, or a fluorescent cluster that is poorly resolved under direct imaging, its size and shape can be identified much more accurately through the second and third moments. Given the results in Refs. [2–4], the interferometric schemes proposed in Refs. [2–4, 46–48] are expected to be similarly useful for estimating the second moments at least. For larger objects, scanning in the manner of confocal microscopy [18] should be useful.

Many open problems remain; chief among them are the incorporation of prior information, generalizations for non-Gaussian PSFs, potential further improvements by alternative measurements, and the derivation of fundamental quantum limits. These are daunting problems, but may be attacked by more advanced methods in quantum metrology [49–52], quantum state tomography [53–55], and compressed sensing [54–56].

Useful discussions with Ranjith Nair, Xiao-Ming Lu, Shan Zheng Ang, Shilin Ng, Laura Waller’s group, Geoff Schiebinger, and Ben Recht are gratefully acknowledged. This work is supported by the Singapore National Research Foundation under NRF Grant No. NRF-NRFF2011-07 and the Singapore Ministry of Education Academic Research Fund Tier 1 Project R-263-000-C06-112.

---

\* mankei@nus.edu.sg

- [1] M. Tsang, R. Nair, and X.-M. Lu, ArXiv e-prints (2015), [arXiv:1511.00552](https://arxiv.org/abs/1511.00552) [quant-ph].
- [2] S. Z. Ang, R. Nair, and M. Tsang, ArXiv e-prints (2016), [arXiv:1606.00603](https://arxiv.org/abs/1606.00603) [quant-ph].
- [3] R. Nair and M. Tsang, *Opt. Express* **24**, 3684 (2016).
- [4] R. Nair and M. Tsang, ArXiv e-prints (2016), [arXiv:1604.00937](https://arxiv.org/abs/1604.00937) [quant-ph].
- [5] M. Tsang, R. Nair, and X.-M. Lu, ArXiv e-prints (2016), [arXiv:1602.04655](https://arxiv.org/abs/1602.04655) [quant-ph].
- [6] M. Tsang, ArXiv e-prints (2016), [arXiv:1605.03799](https://arxiv.org/abs/1605.03799) [quant-ph].
- [7] C. Lupo and S. Pirandola, ArXiv e-prints (2016), [arXiv:1604.07367](https://arxiv.org/abs/1604.07367) [quant-ph].
- [8] J. Rehacek, M. Paur, B. Stoklasa, L. Motka, Z. Hradil, and L. L. Sanchez-Soto, ArXiv e-prints (2016), [arXiv:1607.05837](https://arxiv.org/abs/1607.05837) [quant-ph].
- [9] Z. S. Tang, K. Durak, and A. Ling, ArXiv e-prints (2016), [arXiv:1605.07297](https://arxiv.org/abs/1605.07297) [physics.optics].
- [10] F. Yang, A. Taschilina, E. S. Moiseev, C. Simon, and A. I. Lvovsky, ArXiv e-prints (2016), [arXiv:1606.02662](https://arxiv.org/abs/1606.02662) [physics.optics].
- [11] W. K. Tham, H. Ferretti, and A. M. Steinberg, ArXiv e-prints (2016), [arXiv:1606.02666](https://arxiv.org/abs/1606.02666) [physics.optics].
- [12] M. Paúr, B. Stoklasa, Z. Hradil, L. L. Sánchez-Soto, and J. Rehacek, ArXiv e-prints (2016), [arXiv:1606.08332](https://arxiv.org/abs/1606.08332) [quant-ph].
- [13] E. Bettens, D. Van Dyck, A. J. den Dekker, J. Sijbers, and A. van den Bos, *Ultramicroscopy* **77**, 37 (1999).
- [14] S. Van Aert, A. J. den Dekker, D. Van Dyck, and A. van den Bos, *Journal of Structural Biology* **138**, 21 (2002).
- [15] S. Ram, E. S. Ward, and R. J. Ober, *Proceedings of the National Academy of Sciences of the United States of America* **103**, 4457 (2006).
- [16] D. J. Brady, *Optical Imaging and Spectroscopy* (Wiley, Hoboken, 2009).
- [17] R. J. Prokop and A. P. Reeves, *CVGIP: Graphical Models and Image Processing* **54**, 438 (1992).
- [18] J. B. Pawley, ed., *Handbook of Biological Confocal Microscopy* (Springer, New York, 2006).
- [19] H. Deschout, F. C. Zanacchi, M. Mlodzianoski, A. Diaspro, J. Bewersdorf, S. T. Hess, and K. Braeckmans, *Nature Methods* **11**, 253 (2014).
- [20] K. I. Mortensen, L. S. Churchman, J. A. Spudich, and H. Flyvbjerg, *Nature Methods* **7**, 377 (2010).
- [21] J. Chao, E. Sally Ward, and R. J. Ober, *Journal of the Optical Society of America A* **33**, B36 (2016).
- [22] J. Zmuidzinas, *J. Opt. Soc. Am. A* **20**, 218 (2003).
- [23] M. C. E. Huber, A. Pauluhn, J. L. Culhane, J. G. Timothy, K. Wilhelm, and A. Zehnder, eds., *Observing Photons in Space: A Guide to Experimental Space Astronomy* (Springer, New York, 2013).
- [24] J. W. Goodman, *Statistical Optics* (Wiley, New York, 1985).
- [25] J. H. Shapiro, *IEEE Journal of Selected Topics in Quantum Electronics* **15**, 1547 (2009).
- [26] J. W. Goodman, *Introduction to Fourier Optics* (McGraw-Hill, New York, 2004).
- [27] L. A. Wasserman, *All of Statistics* (Springer, New York, 2004).
- [28] C. W. Helstrom, *J. Opt. Soc. Am.* **60**, 659 (1970).
- [29] L. Motka, B. Stoklasa, M. D’Angelo, P. Facchi, A. Garuccio, Z. Hradil, S. Pascasio, F. V. Pepe, Y. S. Teo, J. Řeháček, and L. L. Sánchez-Soto, *The European Physical Journal Plus* **131**, 130 (2016).
- [30] R. Zamir, *IEEE Transactions on Information Theory* **44**, 1246 (1998).
- [31] A. Yariv, *Quantum Electronics* (Wiley, New York, 1989).
- [32] DLMF, “NIST Digital Library of Mathematical Functions,” <http://dlmf.nist.gov/>, Release 1.0.11 of 2016-06-08, online companion to [33].
- [33] F. W. J. Olver, D. W. Lozier, R. F. Boisvert, and C. W. Clark, eds., *NIST Handbook of Mathematical Functions* (Cambridge University Press, New York, NY, 2010) print companion to [32].
- [34] L. Mandel and E. Wolf, *Optical Coherence and Quantum Optics* (Cambridge University Press, Cambridge, 1995).
- [35] M. Bertero and C. de Mol, in *Progress in Optics*, Vol. 36, edited by E. Wolf (Elsevier, 1996) pp. 129–178.
- [36] M. I. Kolobov, ed., *Quantum Imaging* (Springer, New York, 2007).
- [37] K. Piché, J. Leach, A. S. Johnson, J. Z. Salvail, M. I. Kolobov, and R. W. Boyd, *Opt. Express* **20**, 26424 (2012).
- [38] H. L. Van Trees and K. L. Bell, eds., *Bayesian Bounds for Parameter Estimation and Nonlinear Filtering/Tracking* (Wiley-IEEE, Piscataway, 2007).
- [39] J.-F. Morizur, L. Nicholls, P. Jian, S. Armstrong, N. Treps, B. Hage, M. Hsu, W. Bowen, J. Janousek, and H.-A. Bachor, J.

- [Opt. Soc. Am. A \*\*27\*\*, 2524 \(2010\).](#)
- [40] S. Armstrong, J.-F. Morizur, J. Janousek, B. Hage, N. Treps, P. K. Lam, and H.-A. Bachor, [Nature Commun. \*\*3\*\*, 1026 \(2012\).](#)
- [41] W. E. Moerner, [Proceedings of the National Academy of Sciences \*\*104\*\*, 12596 \(2007\).](#)
- [42] E. Betzig, G. H. Patterson, R. Sougrat, O. W. Lindwasser, S. Olenych, J. S. Bonifacino, M. W. Davidson, J. Lippincott-Schwartz, and H. F. Hess, [Science \*\*313\*\*, 1642 \(2006\).](#)
- [43] S. W. Hell, [Science \*\*316\*\*, 1153 \(2007\).](#)
- [44] R. N. Bracewell, [Nature \*\*274\*\*, 780 \(1978\).](#)
- [45] M. A. C. Perryman, [Reports on Progress in Physics \*\*63\*\*, 1209 \(2000\).](#)
- [46] N. Sandeau and H. Giovannini, [Journal of the Optical Society of America A \*\*23\*\*, 1089 \(2006\).](#)
- [47] K. Wicker and R. Heintzmann, [Optics Express \*\*15\*\*, 12206 \(2007\).](#)
- [48] K. Wicker, S. Sindbert, and R. Heintzmann, [Optics Express \*\*17\*\*, 15491 \(2009\).](#)
- [49] C. W. Helstrom, *Quantum Detection and Estimation Theory* (Academic Press, New York, 1976).
- [50] A. S. Holevo, *Probabilistic and Statistical Aspects of Quantum Theory* (Edizioni della Normale, Pisa, Italy, 2011).
- [51] M. Hayashi, ed., *Asymptotic Theory of Quantum Statistical Inference: Selected Papers* (World Scientific, Singapore, 2005).
- [52] J. Kahn and M. Guță, [Communications in Mathematical Physics \*\*289\*\*, 597 \(2009\).](#)
- [53] A. I. Lvovsky and M. G. Raymer, [Reviews of Modern Physics \*\*81\*\*, 299 \(2009\).](#)
- [54] D. Gross, Y.-K. Liu, S. T. Flammia, S. Becker, and J. Eisert, [Phys. Rev. Lett. \*\*105\*\*, 150401 \(2010\).](#)
- [55] J. Haah, A. W. Harrow, Z. Ji, X. Wu, and N. Yu, ArXiv e-prints (2015), [arXiv:1508.01797 \[quant-ph\]](#).
- [56] G. Schiebinger, E. Robeva, and B. Recht, ArXiv e-prints (2015), [arXiv:1506.03144 \[math.OC\]](#).